

SiHCl. The values of k_6 , k_{7a} , and k_{7b} were therefore averaged over the two Boltzmann distributions, with SiHCl and SiH₄ having average energies of 17 and 4 kcal/mol, respectively.

Fundamental frequencies for Si₂H₅Cl were not available from the literature; therefore, we estimated these frequencies based upon analogous assignments and symmetry constraints for chloroethane⁴⁵ and by combination of various fundamental modes of Si₂H₆,⁴⁰ CH₃SiH₂Cl, CH₃SiHCl₂, CH₂ClSiH₃ and CHCl₂SiH₃.⁴⁰ Table II contains these estimated frequencies for Si₂H₅Cl as well as for the three activated complexes used in calculating k_6 , k_{7a} , and k_{7b} .

Using the energetic values and estimated frequencies just described for the three modes of decomposition of Si₂H₅Cl*, we calculate from RRKM theory that $(k_{7a} + k_{7b})/k_6$ is 17.5, which is to be compared with the value of about 2 that we find experimentally. While the agreement is not particularly good, which is not surprising considering the uncertainties in the frequencies and thermochemistry, it at least tends to confirm the experimental finding that $(k_{7a} + k_{7b}) > k_6$. Moreover, these considerations serve to rationalize the observed increase in $R(\text{CH}_4)/R(\text{SiH}_3\text{Cl})$ with increasing pressure that is seen in Figure 8. At higher total pressures, the Si₂H₅Cl* formed in (5) is more likely to be collisionally deactivated, thus making (6) much less favorable and causing the ratio $R(\text{CH}_4)/R(\text{SiH}_3\text{Cl})$ to increase.

(45) Miller, F. A.; Kiviat, F. E. *Spectrochim. Acta* 1969, 25, 1363.

Experiments to examine the effect of an inert third body on the rate ratio $R(\text{SiH}_3\text{Cl})/R(\text{CH}_4)$ were carried out with the partial pressures of SiH₄ and CH₃Cl kept constant at 40 and 30 Torr, respectively. In these experiments both 20 Torr of SiF₄ and 10 Torr of C(CH₃)₄ were used as third bodies.

Rather surprisingly, the ratio $R(\text{SiH}_3\text{Cl})/R(\text{CH}_4)$ decreased almost to zero; that is, almost no SiH₃Cl was produced. It appears that if sufficient amounts of inert third body are present, the reaction of SiHCl going to the solid phase (nucleation) is enhanced.

This enhancement is explained by our mechanism as follows. The SiHCl which is formed in reaction 4 inserts into the Si-H bond of silane, forming an energized Si₂H₅Cl* which can either decompose by (6) to form SiH₃Cl and regenerate SiH₂ or decompose by (7) to form an Si₂H₅Cl diradical species. The barrier for reaction 6 is higher than that for either reaction 7a or 7b, and only a certain fraction of the Si₂H₅Cl* formed in (5) may contain enough energy to undergo reaction 6. If an adequate amount of third body (either SiF₄ or (Me)₄C) is added, the Si₂H₅Cl* (as well as the SiHCl formed in (4)) is sufficiently collisionally stabilized that there is not enough energy to overcome the activation barrier for reaction 6 and only reactions 7a and 7b can take place.

Acknowledgment. This work was supported by Contract No. DE-ASO2-76ER03416 with the U.S. Department of Energy.

Registry No. SiH₄, 7803-62-5; CH₃Cl, 74-87-3; H₂, 1333-74-0; CH₄, 74-82-8; Si₂H₆, 1590-87-0; SiH₃Cl, 13465-78-6; Si₃H₈, 7783-26-8; CH₃SiH₂Cl, 993-00-0.

Shock Tube Pyrolysis of Pyridine[†]

John C. Mackie,*

Department of Physical Chemistry, University of Sydney, NSW 2006, Australia

Meredith B. Colket III,

United Technologies Research Center, Silver Lane, East Hartford, Connecticut 06108

and Peter F. Nelson

CSIRO Division of Coal Technology, North Ryde, NSW 2113, Australia (Received: May 30, 1989; In Final Form: November 1, 1989)

The kinetics of pyrolysis of pyridine dilute in argon have been studied in a single-pulse shock tube, using capillary column GC together with GC/MS and FTIR spectroscopy for product determination, over the temperature range of 1300–1800 K and total pressures of 7–11 atm. At the lower end of the studied temperatures, cyanoacetylene was found to be the principal nitrogen-containing product. At elevated temperature hydrogen cyanide predominated. Other major products were acetylene and hydrogen. Thermochemical estimates of the isomeric cyclic pyridyls produced in the pyrolysis indicate that the ortho isomer is unique in being able to undergo facile cleavage to an open-chain cyano radical from which cyanoacetylene is produced. Several sources of HCN were identified in the system. The *m*- and *p*-pyridyls may eliminate HCN in a molecular process. An important source of HCN at high temperatures is the addition of H atoms to cyano compounds, especially cyanoacetylene, but also acetonitrile and acrylonitrile which are produced in the pyrolysis. The pyrolysis is a chain process initiated principally by C–H bond fission to form *o*-pyridyl. A 58-step reaction model is presented and shown to substantially fit the observed profiles of the major product species. From this model we derive a value for the rate constant of the principal initiation reaction, C₅H₅N → *o*-C₅H₄N + H (1), of $k_1 = 10^{15.9 \pm 0.4} \exp(-98 \pm 3 \text{ kcal mol}^{-1}/RT) \text{ s}^{-1}$ between 1300 and 1800 K and at a total pressure of about 10 atm.

Introduction

Heavy fuels such as coal and coal-derived liquids contain considerable amounts of chemically bound nitrogen and the combustion of these fuels can lead to significant amounts of fuel-derived NO_x.¹⁻³ Much of the nitrogen originally bound in the fuel is in the form of aromatic heterocyclic structures containing pyridine and pyrrole ring systems.^{4,5} Under pyrolytic

conditions these heterocycles may form nitrogen precursors of NO_x so that the rates of pyrolysis and product formation from representative nitrogen heterocycles will determine NO_x formation in the combustion of heavy fuels.

(1) Pershing, D. W.; Wendt, J. O. L. *Sixteenth Symposium (International) on Combustion*; the Combustion Institute: Pittsburgh, PA, 1977; p 389.

(2) Painter, P. C.; Coleman, M. M. *Fuel* 1979, 58, 301.

(3) Turner, D. W.; Andrews, R. L.; Siegmund, C. W. *AIChE Symp. Ser.* 1972, 68, No. 126, 55.

(4) Snyder, L. R. *Anal. Chem.* 1969, 41, 314.

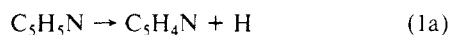
(5) Brandenburg, C. F.; Latham, D. R. *J. Chem. Eng. Data* 1968, 13, 391.

[†] Presented in part as a Poster Paper at 21st Symposium (International) on Combustion, Seattle, August 1988.

The thermal decomposition of pyridine has been studied previously⁶⁻⁸ in flow systems between 1100 and 1400 K. Acetylene and hydrogen cyanide have been found to be major products. Other nitrogen-containing products have been identified as acrylonitrile, benzonitrile, quinoline, and acetonitrile, although dispute exists^{7,8} over the observation of acetonitrile.

Axworthy et al.⁷ found that the decomposition of pyridine followed first-order kinetics with an overall rate constant of $3.8 \times 10^{12} \exp(-70 \text{ kcal mol}^{-1}/RT) \text{ s}^{-1}$ between 1100 and 1200 K. Houser et al.⁸ found that the decomposition kinetics were complex and did not follow first-order kinetics exactly. However, they derived an approximate first-order rate constant of $1 \times 10^{12} \exp(-75 \text{ kcal mol}^{-1}/RT) \text{ s}^{-1}$, about an order of magnitude lower than that of Axworthy et al.

Recently, Kern et al.⁹ carried out a shock tube study of the pyrolysis of pyridine over the temperature range of 1700–2400 K and at pressures between 0.2 and 0.5 atm using both laser schlieren densitometry and time-of-flight mass spectrometry as diagnostic tools. They proposed a chain mechanism with first-order initiation involving a ring hydrogen fission



with a specific pressure-dependent rate constant of $1.08 \times 10^{12} \exp(-74.5 \text{ kcal mol}^{-1}/RT) \text{ s}^{-1}$. In their analysis the $\text{C}_5\text{H}_4\text{N}$ represented a weighted average of the isomeric pyridyl radicals. From a RRKM extrapolation of their rate data, Kern et al. derived an average value of $76 \pm 10 \text{ kcal mol}^{-1}$ for the heat of formation of the pyridyl radicals, a value higher than that implied by the earlier flow studies.⁶⁻⁸

In a recent shock tube study Leidreiter and Wagner¹⁰ measured the rate of decomposition of pyridine at temperatures between 1700 and 2000 K and at total densities of 2×10^{-6} to $3 \times 10^{-5} \text{ mol cm}^{-3}$, using time-resolved absorption measurements at 279 nm. They did not determine products but from falloff curves they were able to extrapolate their rate data to obtain the limiting high-pressure rate constant for disappearance of pyridine of $k_{\infty} = 10^{16.2} \exp(-100 \text{ kcal mol}^{-1}/RT) \text{ s}^{-1}$.

The lower reported values of the activation energy of the initiation step (70–75 kcal mol⁻¹) imply that the C–H bond energy in pyridine is considerably lower than that in benzene (assuming that the initiation step is C–H fission). Also, Kern et al.⁹ detected only one nitrogen-containing product, hydrogen cyanide, although in flow studies several other nitrogen products were observed. Thus, the present shock tube kinetic study of pyridine pyrolysis, using capillary column gas chromatography and gas chromatography/mass spectrometry for detection, is oriented toward detailed product identification and elucidation of the pyrolysis mechanism.

Experimental Section

Pyrolyses were carried out on two single-pulse shock tubes, one of diameter 3.8 cm at UTRC was primarily used for kinetic studies, and the other, at the University of Sydney (diameter 7.6 cm), was used principally for product identification in conjunction with FTIR and a GC/MS at CSIRO. Both shock tubes are basically similar; the UTRC tube and on-line capillary GC analytical system have been described previously.¹¹

Pyridine samples were purchased from Aldrich (HPLC grade) and from Merck (A.R. grade). Further purification by several bulb-to-bulb distillations produced pyridine samples of purity

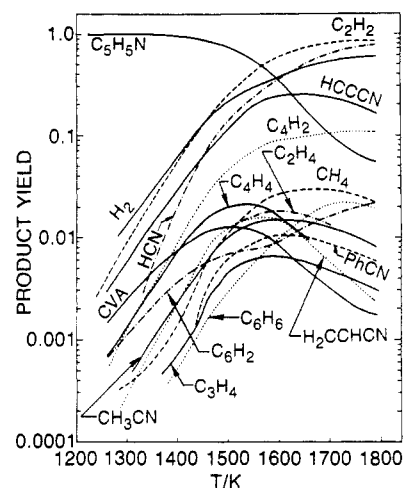


Figure 1. Distribution of all products of significance behind reflected shocks in the 0.7% pyridine in argon mixture over the temperature range studied.

exceeding 99.9% (by GC with CH_3CN as the only detectable impurity). No difference between the two sources of pyridine was observed.

For the kinetic studies, mixtures of 0.7 and 0.15% pyridine in argon were prepared and stored in glass bulbs. Pressures and temperatures behind the reflected shock were computed from the measured incident shock velocity. Residence times and quenching rates by the rarefaction wave were measured from pressure profiles recorded by Kistler gauges. Reflected shocked gas temperatures ranged from 1200 to 1800 K and total pressures from 7 to 11 atm. Residence times at uniform temperatures behind the reflected shock front ranged from 450 to 600 μs . For the product analyses, three separate capillary GC columns were used. The UTRC shock tube was equipped with a Chrompack CP Sil 5 capillary column. The Sydney shock tube employed a SGE BP-1 (5 μm bonded phase dimethylsiloxane) wide-bore column whereas the CSIRO GC/MS was equipped with an SGE BP-1 0.5- μm bonded phase.

Where commercial samples were available, product identification and calibration were made from capillary GC retention times and areas by direct comparison with standards. HCN was purchased as a standard mixture in N_2 from Scott Specialty Gases. Acetonitrile, acrylonitrile, and benzonitrile (all >99% purity) were obtained from Aldrich. C_1 – C_6 hydrocarbons were calibrated gas standards prepared and analyzed by Scott Environmental Laboratories.

Cyanoacetylene (HCCCN) was identified in the product gases by FTIR absorption spectroscopy in a 7-m cell (via its strong CCH bend at 663.4 cm^{-1} and the CN stretch at 2272 cm^{-1}). Product samples from the Sydney shock tube were collected in gas burets and transported to CSIRO for GC/MS analysis. The GC peak assigned to cyanoacetylene was confirmed not only by the observation of the parent peak at 51 amu, but also through the observation of its fragmentation pattern whose intensities were in excellent agreement with those reported by Dibeler et al.¹²

Other products confirmed both by FTIR and GC/MS were hydrogen cyanide, vinylacetylene, and diacetylene. In addition, triacetylene (C_6H_2) and cyanodiacetylene (HC_5N) were positively identified by GC/MS.

Both hydrocarbons and nitrogen-containing compounds were detected by a flame ionization detector (fid) the sensitivity of HCN, however, was only about one-tenth that of C_2H_2 , permitting measurements of HCN to be made with adequate precision above about 30 ppm. Hydrogen was detected by TCD.

The capillary column/sampling system exhibited a “memory effect” for the nitrogen-containing compounds, especially pyridine, benzonitrile, acetonitrile, and acrylonitrile. Repeatability of in-

(6) Hurd, C. D.; Simon, J. I. *J. Am. Chem. Soc.* **1962**, *84*, 4519.

(7) Axworthy, A. E.; Dayan, V. H.; Martin, G. B. *Fuel* **1978**, *57*, 29.

(8) Houser, T. J.; McCarville, M. E.; Biftu, T. *Int. J. Chem. Kinet.* **1980**, *12*, 555.

(9) Kern, R. D.; Yong, J. N.; Kiefer, J. H.; Shah, J. N. Shock Tube Studies of Pyridine Pyrolysis and their Relation to Soot Formation. Paper presented at 16th International Symposium on Shock Tubes and Waves, 1987.

(10) Leidreiter, H. I.; Wagner, H. G. *Z. Phys. Chem. N. F.* **1987**, *153*, 99.

(11) Colket, M. B. *Shock Tubes and Waves; Proceedings of the 15th International Symposium*; Stanford University Press: Stanford, CA, 1986; p 311.

(12) Dibeler, V. H.; Reese, R. M.; Franklin, J. L. *J. Am. Chem. Soc.* **1961**, *83*, 1813.

TABLE I: Thermochemical Parameters for the Pyridine System

species	$\Delta H_f^\circ_{300}$, kcal mol ⁻¹	S°_{300} , cal mol ⁻¹ K ⁻¹	C_p , cal mol ⁻¹ K ⁻¹				
			300	500	1000	1500	2000
C ₅ H ₅ N	33.48 ^a	69.99	18.70	30.85	46.56	53.14	56.27
C ₅ H ₄ N	91.7 ^b	72.6	18.0	28.9	42.8	48.5	51.1
I ^c	114 ± 3	79	23.6	32.6	43.1	48.2	50.8
II ^c	142 ± 6						
III ^c	152 ± 6						
HCCCN	84.6 ^d	56.54	15.48	18.66	22.38	24.24	25.19
HC=CHCN	97 ± 3	64.7	15.9	19.8	25.3	27.8	29.3
H ₂ CCHCN	43.9 ^e	65.32	15.26	20.93	28.90	32.66	34.53
CVA ^f	99.5	76.92	22.53	30.17	39.55	43.82	45.99
HC ₃ N	142	73.91	22.45	27.03	32.54	35.21	36.52
c-C ₄ H ₃ NCH ₃ ^g	46.4	77.5	20.3	32.3	48.6	58.2	62.7
groups							
C _d -(H)(CN)	37.6	37.7	10.12	13.47	17.67	19.48	20.38
C _f -(CN)	57.7	31.8	10.20	12.11	14.31	15.28	15.71
N _i	76 ± 5						

^a Reference 33. ^b For *o*- and *p*-pyridyls, add -1.5 kcal mol⁻¹ (see Ref 10). ^c For structures of these open-chain radicals from pyridyls, see Figure 2. $\Delta H_f^\circ_{300}$ values have been estimated for all other possible open-chain radicals from pyridyls and are all >150 ± 6 kcal mol⁻¹. ^d Reference 34. ^e Reference 35. ^f CVA = cyanovinylacetylene, HC≡C-CH=CH-CN. ^g c-C₄H₃NCH₃ = methylpyrrolyl.

jections of these compounds was only ±10%. Pyridine mixtures in argon slowly decreased in concentration with storage, requiring frequent recalibrations.

Adsorption and/or polymerization of the product cyano compounds on to the walls of the gas burets was a problem leading to significant losses in sensitivity of these products in transportation of samples for GC/MS analyses.

Results

Yields of all products of significance (scaled by the initial concentration of pyridine) are shown in Figure 1 as a function of temperature for the 0.7% mixture of pyridine in argon. The variation of pyridine concentration with temperature is also given in Figure 1.

The principal hydrocarbon product at all temperatures and for both series of mixtures was acetylene. Hydrogen was an important product at all temperatures. The C₂H₂/H₂ ratio varied from about 1/3 at 1300 K to about 1.5/1 at 1800 K. At the lower end of the studied temperature range, cyanoacetylene was the principal nitrogen-containing product, being higher in yield than HCN by about a factor of 2. From FTIR difference spectra of the products from successive runs in the lower range of temperatures it was shown that the rates of increase with temperature of both acetylene and cyanoacetylene were approximately equal. With increasing temperature HCN yields overtook those of HCCCN such that the yield of HCN is about 4 times that of HCCCN at 1800 K. Much smaller yields of acetonitrile and acrylonitrile were recorded at all temperatures. An additional product was detected and was assumed to be a cyano-containing species due both to the characteristic tailing of the GC peak that this class of compounds exhibits on the capillary column and also to the lack of appearance of this peak during pyrolysis of pure hydrocarbons. This product peaked in yield at about 1500 K and was present even at the lowest temperature at which decomposition could be detected. From its retention time, eluting just after C₆H₂, which, in turn, eluted soon after HC₃N, it has been tentatively assigned as cyanovinylacetylene (β -ethynylacrylonitrile, HC≡C-CH=CHCN). Attempts to confirm this assignment by GC/MS were unsuccessful, however, as the level of this peak after transportation of the product gases for analysis had dropped below sensitivity limits. Cyanovinylacetylene is known to polymerize rapidly¹³ above -30 °C.

Other products included vinylacetylene (C₄H₄), important at the lower temperatures, diacetylene and triacetylene, important over the entire temperature range, methane, ethylene, and benzene. There were also significant yields of benzonitrile, allene, and/or propyne (unresolved by the capillary columns) together with traces of propene, butadiene, styrene, and phenylacetylene. Cyanodi-

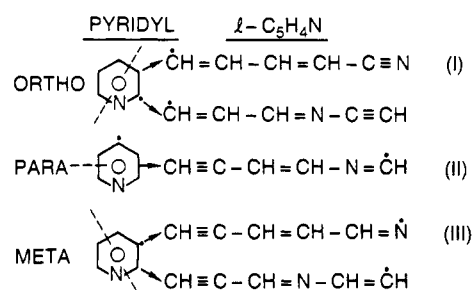


Figure 2. Possible open-chain radicals arising from simple ring cleavage of pyridyls.

acetylene (HC₃N) yields only became significant at the higher temperatures of this study.

When results from the two series of initial pyridine concentrations (0.7% and 0.15%) were compared, it was found that the overall decomposition of pyridine and formation of major products HCN, C₂H₂, HCCCN, and H₂ were essentially independent of initial pyridine concentration. This independence upon initial pyridine concentration was also observed for products C₄H₄, CH₄, and acrylonitrile. Thus, overall first-order kinetics are observed for pyridine decomposition, and for the formation of the major as well as many of the minor species. The first-order behavior is consistent with that previously observed.⁷ Because of the first-order behavior it is convenient in reporting species data to present normalized concentrations of reactant and products in Figures 1 and 3-6.

Discussion

Thermochemistry of the Pyridine System. The reaction mechanism developed to interpret the above results involves a chain reaction initiated by C-H bond scission, as suggested previously. Subsequent reactions are dependent on the thermochemistry of the cyclic pyridyl radicals produced by the scission. The enthalpies of formation of the pyridyls were estimated under the assumption that the C-H bond energy in pyridine was equal to that in benzene together with a stabilization energy¹⁴ of 1.5 kcal mol⁻¹ for the *o*- and *p*-pyridyls. Using the assumption of equality of C-H bond energies of pyridine and benzene, Dewar and co-workers^{15a,b} have calculated enthalpies of atomization of pyridine and other molecules containing the pyridine ring, in very good agreement with experiment by SCF MO techniques. Heat capacities and entropies of the pyridyls have been estimated by group additivity methods¹⁴

(14) Benson, S. W.; Cruikshank, F. R.; Golden, D. M.; Haugen, G. R.; O'Neal, H. E.; Rodgers, A. S.; Shaw, R.; Walsh, R. *Chem. Rev.* **1969**, *69*, 279.

(15) (a) Dewar, M. J. S.; Morita, T. *J. Am. Chem. Soc.* **1969**, *91*, 796. (b) Dewar, M. J. S.; Harget, A. J.; Trinajstić, N. *J. Am. Chem. Soc.* **1969**, *91*, 6321.

(13) August, J.; Kroto, H. W.; McNaughton, D.; Phillips, K.; Walton, D. R. M. *J. Mol. Spectrosc.* **1988**, *130*, 424.

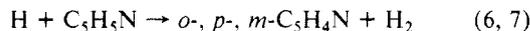
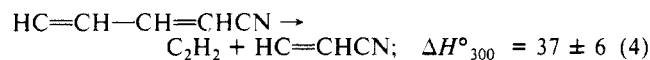
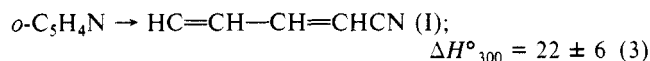
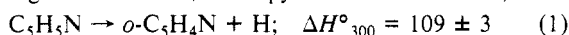
by assuming that the contribution of the C_B group to the pyridyl thermochemistry was equal to that in phenyl.

All pyridyl radicals may undergo thermal ring fission. However, the *o*-pyridyl is unique in its ability to produce directly an open-chain cyano radical (I). Figure 2 shows all possible open-chain "linear" radicals 1-C₅H₄N arising from simple ring cleavage. As the values in Table I indicate, the cyano radical (I) should be overwhelmingly more stable than any other open-chain radical produced by ring fission of pyridyls.

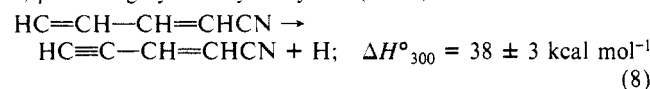
Because of the lack of thermochemical data for the pyridyls we have had to resort to approximate group additivity methods to arrive at the estimates of the thermochemical parameters given in Table I. To estimate thermochemical parameters for radical I, thermochemical data for group C_d-(H)(CN) were obtained by additivity methods¹⁴ from the acrylonitrile thermochemistry together with data for *n*-C₄H₅^{*} (ref 16). Estimates for radical II were calculated from the thermochemistry of CH=NH, 1-C₆H₅, and C₂H₃ (ref 16). Thermochemical data for CH=NH were calculated by Melius using the BAC-MP4 technique.¹⁷ The enthalpy of formation of 1-C₆H₅ was estimated by additivity methods¹⁸ and the value of $\Delta H_f^\circ_{300} = 139 \text{ kcal mol}^{-1}$ used in the present work compares well with a recent determination by Braun-Unkoff et al.¹⁹ of $144 \pm 3 \text{ kcal mol}^{-1}$. N₁ group data (required for radical (III)) were estimated by comparing group differences between >C=CH and >C=CH₂ with >C=N and >C=NH where N₁-(H) data are available from CH₂=NH. The enthalpy of formation of CH₂=NH has been measured experimentally.²⁰ Heat capacities and entropies are obtained from spectroscopy.²¹

Thermochemical data for HCCCN, HC₅N, and H₂C=CHCN were computed by statistical methods using molecular constants from refs 22–24. Other relevant group data are available in the thermochemistry literature.^{14,25}

Reaction Mechanism. Based on the assumption of the stability of the open-chain cyano radical (I), the dominant mechanism in the pyrolysis of pyridine in the lower end of the studied temperature range of 1300–1800 K is postulated to be (reaction numbering as in Table II; enthalpy values in kcal mol⁻¹):



This is the major low-temperature chain mechanism, although a minor chain process may arise via fission of a secondary H from I, producing cyanovinylacetylene (CVA).



(16) Weissmann, M. A.; Benson, S. W. *J. Phys. Chem.* **1988**, *92*, 4080. Revised vinyl radical thermochemistry presented in this reference is used in the present work.

(17) Melius, C. F. "BAC-MP₄ Heats of Formation and Free Energies"; Sandia National Laboratories, Livermore, July 1986.

(18) Colket, M. B. *Twenty-First Symposium (International) on Combustion*; the Combustion Institute: Pittsburgh, PA, 1986; p 851.

(19) Braun-Unkoff, M.; Frank, P.; Just, T. *Twenty-Second Symposium (International) on Combustion*; the Combustion Institute: Pittsburgh, PA, 1988; p 1053.

(20) (a) De Frees, D. J.; Hehre, W. J. *J. Phys. Chem.* **1978**, *82*, 391. (b) Grela, M. A.; Colussi, A. J. *Int. J. Chem. Kinet.* **1988**, *20*, 713.

(21) Jacox, M. E.; Milligan, D. E. *J. Mol. Spectrosc.* **1975**, *56*, 333.

(22) Job, V. A.; King, G. W. *J. Mol. Spectrosc.* **1966**, *19*, 155.

(23) Alexander, A. J.; Kroto, H. W.; Walton, D. R. M. *J. Mol. Spectrosc.* **1976**, *62*, 175.

(24) (a) Costain, C. C.; Stoicheff, B. P. *J. Chem. Phys.* **1959**, *30*, 777. (b) Kamesaka, I.; Miyawaki, K.; Kawai, K. *Spectrochim. Acta* **1976**, *32A*, 195.

(25) Kee, R. J.; Ruley, F. M.; Miller, J. A. "The Chemkin Thermodynamic Data Base"; Sandia Report SAND87-8215, April, 1987.

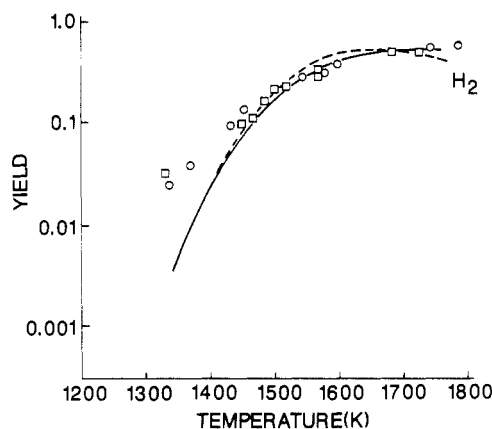


Figure 3. Comparison between the simulated yield of the designated product (lines) and experimental yields (symbols): — and O, 0.7% mixture; --- and □, 0.15% mixture of pyridine in argon.

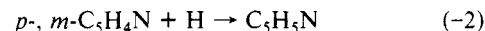
The HCCHCN radical was found to decompose principally via reaction 5. Other possibilities include



but the larger endothermicities of these reactions make them less likely at least in the lower temperatures of this study.

The above short-chain mechanism is in accord with the experimental observations that HCCCN is the principal nitrogen-containing product at low temperatures, and of the equivalence in production rates of C₂H₂ and HCCCN. It also gives an explanation for the product peak (assigned as CVA) which appears at low temperatures.

The thermochemistry of the *m*- and *p*-pyridyls suggests that these radicals will be stable with respect to simple ring cleavage, hence the reverse of reaction 2



terminates radicals. However, both of these isomers may also undergo molecular elimination of HCN to produce the *n*-C₄H₃ radical (reaction 9). There are other possible sources of HCN. Open-chain radical I could eliminate HCN in a molecular process involving a cyclic transition state (reaction 10). Although we are unaware of any previous studies of HCN elimination from cyclic radicals, Braun-Unkoff et al.¹⁹ have analyzed the decomposition of benzyl radicals by invoking a rearrangement to a bicyclic C₇H₇^{*} radical which can molecularly eliminate C₂H₂ in an analogous process to our HCN elimination.

At elevated temperatures where high concentrations of H atoms exist, an important source of HCN arises from the addition of H atoms to cyano compounds. The most important of these is reaction -27 which leads to the decay of HCCCN at high temperatures. The abstraction reaction of CN with H₂ also plays a significant role at elevated temperatures.

The detailed reaction mechanism postulated to simulate the yields of the major products is presented in Table II. In addition to the nitrogen chemistry, the mechanism includes acetylene and benzene formation reactions as subsets. For many of the reactions involving nitrogen-containing species, few or no rate constant evaluations are available in the literature. For these reactions estimates were made by using rate constants from analogous reactions or thermochemistry. Based on reaction path analyses and sensitivity analyses, selected rate constants were adjusted to fit the experimental data. These latter rate constants are denoted "PW" in Table II.

For simplification, only one C₄H₃ radical is considered and this is taken to be the normal radical whose $\Delta H_f^\circ_{300}$ is assumed to be 125 kcal mol⁻¹. Allene/propyne is considered to be propyne, the more thermodynamically favored form of C₃H₄ at high temperatures. The reaction model includes, in addition to the short-chain mechanism referred to previously, secondary reactions of the product species and radical-radical reactions. There appear

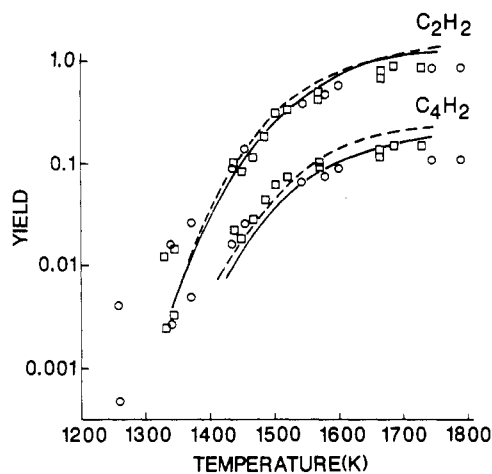


Figure 4. Comparison between the simulated yield of the designated product (lines) and experimental yields (C_2H_2 and C_4H_2). Symbols as in Figure 3.

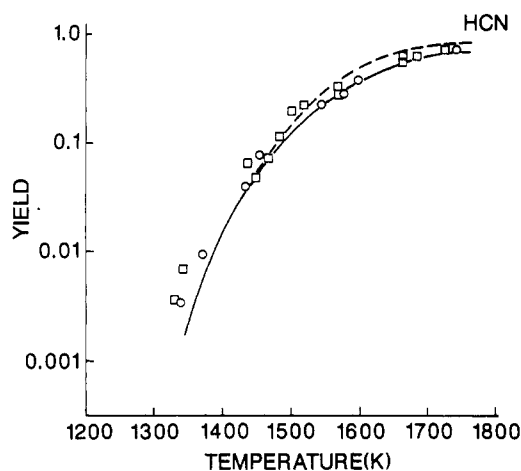


Figure 5. Comparison between the simulated yield of the designated product (lines) and experimental yields (HCN). Symbols as in Figure 3.

to be strong parallels between the addition reactions of acetylene and those of cyanoacetylene. Thus rate constants for radical additions to HCCCN have been chosen by analogy with literature constants for additions to C_2H_2 . Also, acrylonitrile should be able to undergo 2,2 and 3,3 eliminations of HCN and H_2 , respectively, analogous to the 1,1 elimination of H_2 and vinylidene formation reactions of ethylene and vinylacetylene.²⁶ Integration of the kinetic equations was made using the CHEMKIN package,^{27a} LSODE,^{27b} and the SANDIA shock tube code^{27c} which was modified to account for the effects of quenching. Rate of production and sensitivity analyses were carried out by the SENKIN code.²⁸

Comparison of the kinetic model with experiment is given in Figures 3–6 for the major products (i.e., species whose yields are ≥ 0.1 over the studied temperature range). The model adequately describes the temperature dependence of the major products and minor products also from both series of runs. The model also reproduces the experimental pyridine profiles up to about 80% decomposition. Although about 5% of the initial pyridine remains

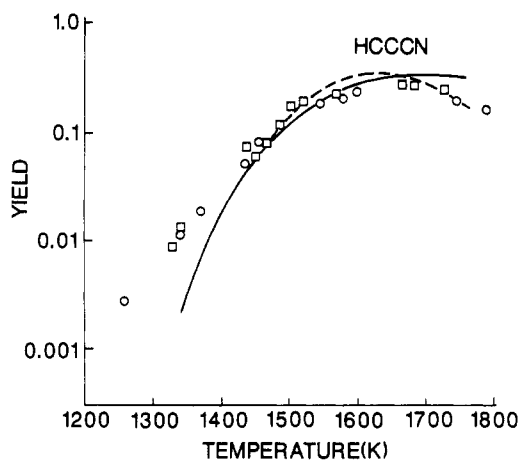
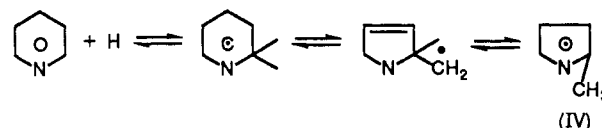


Figure 6. Comparison between the simulated yield of the designated product (lines) and experimental yields (HCCCN). Symbols as in Figure 3.

unreacted due to boundary layer effects at 1800 K, this has little effect on the profiles of the major species. For example, a decrease of about 5% in the HCN concentration at 1800 K is well within our experimental error.

It should be noted that the mechanism of Table II contains certain reactions postulated to simulate minor products' formation. Rate constants were determined based on best fits to experimental data and/or estimates as necessary. In particular, CH_4 , allene/propyne and acetonitrile were observed experimentally in appreciable yields at quite low temperatures, implying their formation through reactions of low activation energy. To simulate the formation of these minor products, a route of low activation energy via H addition to pyridine has been postulated. Reactions 30 and 31 are actually a simplification for a complex addition and ring contraction mechanism:



The methylpyrrolyl radical (IV) produced in the above scheme should possess considerable resonance stability as it is analogous to the methylcyclopentadienyl radical. The group additivity estimate for $\Delta H_f^\circ(IV) = 46 \text{ kcal mol}^{-1}$ (Table I). The methylpyrrolyl may thus be formed in a chemically activated state. It is further suggested that IV may undergo rapid unimolecular reaction to CH_3CN and propargyl radical (C_3H_3). Methane can then arise from methyl radicals produced by reaction of CH_3CN with H (reaction 29). Propargyl radicals are an important source of the C_3H_4 . The proposed reaction scheme to IV is analogous to an addition and ring contraction mechanism postulated by Ritter, Bozzelli, and Dean²⁹ for H addition to benzene and might be regarded as controversial. Nevertheless, these and other reactions of the mechanism postulated to simulate formation of the minor species have only a slight effect on the major products' profiles and have been included solely for completeness.

A brief selection of results of sensitivity analyses of the reaction mechanism is given in Table III. This table contains normalized sensitivity coefficients evaluated at 1600 K and at 100 μs for the mixture of 0.7% pyridine in argon. The accuracy and usefulness of a sensitivity analysis is dependent strongly on the validity of the selected mechanism as well as the specific rate constants. Considering that this detailed chemical kinetic model of pyridine decomposition is the first to describe the formation of cyanoacetylene and several other important nitrogen-containing products

(26) Kiefer, J. H.; Mitchell, K. I.; Kern, R. D.; Yong, J. N. *J. Phys. Chem.* **1988**, *92*, 677.

(27) (a) Kee, R. J.; Miller, J. A.; Jefferson, T. H. "Chemkin: A General-Purpose, Problem-Independent Transportable Fortran Chemical Kinetics Code Package"; Sandia Report SAND80-8003, March 1980. (b) Hindmarsh, A. C. "LSODE and LSODI: Two New Initial Value Differential Equation Solvers", ACM Sigum Newsletter 15 [4], 1980. (c) Mitchell, R. E. and Kee, R. J. "A General-Purpose Computer Code for Predicting Chemical Kinetic Behavior Behind Incident and Reflected Shocks"; Sandia National Laboratories SAND 82-8205, March 1982.

(28) Lutz, A. E.; Kee, R. J.; Miller, J. A. "Senkin: A Fortran Program Predicting Homogeneous Gas Phase Chemical Kinetics with Sensitivity Analysis". Sandia Report SAND87-8248, February 1988.

(29) Ritter, E. R.; Bozzelli, J. W.; Dean, A. M. "Mechanisms of CH_4 , Cyclopentadiene, Biphenyl, Chlorobiphenyl, Toluene and Naphthalene Formation from Pyrolysis of Chlorobenzene in H_2 "; Paper presented at Eastern States Meeting of the Combustion Institute, Washington, DC, November 1987.

TABLE II: Reaction Model for Pyridine Pyrolysis^a

reactions ^c	forward reaction			reverse reaction			ref
	log <i>A</i>	<i>n</i>	<i>E</i>	log <i>A</i>	<i>n</i>	<i>E</i>	
1. C ₅ H ₅ N = <i>o</i> -C ₅ H ₄ N + H	15.90	0.0	98.0	14.10	0.0	-9.8	PW
2. C ₅ H ₅ N = C ₅ H ₄ N + H	15.48	0.0	102.0	13.67	0.0	-7.3	PW
3. <i>o</i> -C ₅ H ₄ N = C ₄ H ₄ CN	14.00	0.0	25.0	11.74	0.0	-0.3	est
4. C ₄ H ₄ CN = C ₂ H ₂ + HCCHCN	13.18	0.0	37.0	11.49	0.0	3.7	PW
5. HCCHCN = HCCCN + H	15.90	0.0	40.0	16.14	0.0	0.2	PW
6. C ₅ H ₅ N + H = <i>o</i> -C ₅ H ₄ N + H ₂	13.48	0.0	5.0	12.29	0.0	1.6	PW
7. C ₅ H ₅ N + H = C ₅ H ₄ N + H ₂	13.70	0.0	9.0	12.51	0.0	4.1	PW
8. C ₄ H ₄ CN = CVA + H	12.00	0.0	40.0	11.30	0.0	3.2	est
9. C ₅ H ₄ N = HCN + C ₄ H ₃	14.48	0.0	57.0	9.65	0.0	-4.8	PW
10. C ₄ H ₄ CN = HCN + C ₄ H ₃	13.70	0.0	45.0	11.13	0.0	7.1	PW
11. C ₄ H ₄ CN = C ₂ H ₃ + HCCCN	12.70	0.0	37.0	10.98	0.0	4.3	PW
12. H + HCCHCN = H ₂ CCHCN	13.30	0.0	0.0	14.60	0.0	104.6	est
13. C ₂ H ₂ + HCN = H ₂ CCHCN	13.48	0.0	40.0	15.08	0.0	80.0	est
14. H + H ₂ CCHCN = HCCHCN + H ₂	13.70	0.0	8.0	13.02	0.0	7.8	est
15. HCCHCN = C ₂ H ₂ + CN	17.90	0.0	58.0	16.50	0.0	0.4	PW
16. C ₄ H ₄ CN = VA + CN	14.70	0.0	59.0	13.01	0.0	4.6	PW
17. CN + H ₂ = HCN + H	13.88	0.0	0.0	14.35	0.0	17.9	36
18. CN + C ₂ H ₂ = C ₂ H + HCN	12.70	0.0	3.0	12.45	0.0	0.6	est
19. H + H ₂ CCHCN = HCN + C ₂ H ₃	13.00	0.0	4.0	11.12	0.0	4.4	est
20. H ₂ CCHCN = HCCCN + H ₂	14.00	0.0	80.0	13.56	0.0	40.0	est
21. CVA + H = C ₂ H ₂ + HCCHCN	13.00	0.0	4.0	12.02	0.0	7.6	est
22. C ₄ H ₃ + C ₅ H ₅ N = <i>o</i> -C ₅ H ₄ N + VA	12.30	0.0	8.0	12.47	0.0	6.0	est
23. C ₄ H ₃ + C ₅ H ₅ N = C ₅ H ₄ N + VA	12.30	0.0	10.0	12.47	0.0	6.5	est
24. CH ₃ + C ₅ H ₅ N = <i>o</i> -C ₅ H ₄ N + CH ₄	11.70	0.0	10.0	11.98	0.0	7.2	est
25. CH ₃ + C ₅ H ₅ N = C ₅ H ₄ N + CH ₄	11.70	0.0	11.5	11.98	0.0	7.2	est
26. CVA + H = HCN + C ₄ H ₃	13.00	0.0	4.0	11.13	0.0	2.9	est
27. C ₂ H + HCN = HCCCN + H	12.30	0.0	0.0	14.19	0.0	20.2	est
28. C ₂ H + HCCCN = C ₄ H ₂ + CN	12.85	0.0	3.0	12.34	0.0	0.3	PW
29. CH ₃ CN + H = HCN + CH ₃	13.70	0.0	2.0	12.22	0.0	10.2	PW
30. H + C ₅ H ₅ N = <i>c</i> -C ₄ H ₃ NMe	12.30	0.0	2.0	12.12	0.0	41.1	PW
31. <i>c</i> -C ₄ H ₃ NMe = CH ₃ CN + C ₃ H ₃	14.70	0.0	60.0	11.02	0.0	7.4	PW
32. C ₃ H ₃ + H = C ₃ H ₄ P	12.70	0.0	0.0	15.24	0.0	89.1	44
33. 2C ₃ H ₃ = C ₂ H ₂ + VA	12.70	0.0	0.0	13.68	0.0	38.2	est
34. CH ₃ + C ₃ H = C ₃ H ₄ P	12.70	0.0	0.0	16.28	0.0	115.6	est
35. C ₄ H ₃ = C ₂ H ₂ + C ₂ H	14.48	0.0	57.0	13.71	0.0	1.7	18
36. C ₄ H ₃ = C ₄ H ₂ + H	12.00	0.0	46.0	12.37	0.0	5.8	PW
37. C ₂ H + H ₂ = H + C ₂ H ₂	12.85	0.0	0.0	13.57	0.0	20.2	37
38. C ₂ H + C ₃ H ₂ = C ₄ H ₂ + H	12.00	0.0	0.0	13.14	0.0	15.1	38 ^b
39. C ₂ H + C ₄ H ₂ = C ₆ H ₂ + H	12.70	0.0	0.0	14.03	0.0	14.8	PW
40. H + C ₂ H ₂ = C ₂ H ₃	12.64	0.0	2.4	12.37	0.0	42.8	39 ^c
41. H + C ₂ H ₄ = C ₂ H ₃ + H ₂	13.70	0.0	8.0	11.87	0.0	6.9	16 ^d
42. CH ₃ + H ₂ = CH ₄ + H	2.81	3.0	7.7	15.14	0.0	17.3	40
43. C ₂ H + C ₂ H ₃ = VA	13.00	0.0	0.0	16.01	0.0	120.8	est
44. C ₂ H ₄ = C ₂ H ₂ + H ₂	17.41	0.0	79.3	15.86	0.0	37.8	40
45. C ₄ H ₃ + C ₂ H ₂ = <i>l</i> -C ₆ H ₅	12.00	0.0	3.0	14.15	0.0	36.9	18
46. <i>l</i> -C ₆ H ₅ = C ₆ H ₅	10.30	0.0	1.4	13.65	0.0	65.2	18
47. C ₆ H ₆ = H + C ₆ H ₅	15.70	0.0	107.9	13.10	0.0	-2.8	41
48. C ₂ H ₃ + C ₄ H ₂ = <i>l</i> -C ₆ H ₅	12.00	0.0	3.0	14.06	0.0	36.7	18
49. 2C ₆ H ₅ = C ₁₂ H ₁₀	12.48	0.0	0.0	16.47	0.0	107.5	42
50. C ₆ H ₆ + H = C ₆ H ₅ + H ₂	14.40	0.0	16.0	12.42	0.0	9.8	43
51. 2C ₃ H ₃ = <i>l</i> -C ₆ H ₆	12.70	0.0	0.0	14.95	0.0	57.8	44
52. <i>l</i> -C ₆ H ₆ = C ₆ H ₆	12.00	0.0	33.0	16.87	0.0	116.0	44
53. C ₄ H ₄ CN + C ₂ H ₂ = C ₆ H ₆ CN	12.70	0.0	1.2	14.57	0.0	37.2	est
54. C ₆ H ₆ CN = <i>c</i> -C ₆ H ₆ CN	11.30	0.0	0.0	14.22	0.0	49.7	est
55. BZN + H = <i>c</i> -C ₆ H ₆ CN	13.60	0.0	2.4	13.56	0.0	26.0	est
56. 2C ₂ H ₂ = VA	13.77	0.0	44.6	15.17	0.0	81.1	26
57. VA = H ₂ + C ₄ H ₂	14.32	0.0	87.0	13.34	0.0	45.4	26
58. C ₂ H + HCCCN = HC ₃ N + H	12.00	0.0	0.0	11.98	0.0	15.3	est

^aUnits for *A*, cm³ mol⁻¹ s. Units for *E*, kcal mol⁻¹. PW indicates rate constant evaluated in present work. est indicates rate constant was estimated in present work. ^bReverse rate constant agrees with value given in reference at 1600 K. ^cFalloff value. Pressure dependence as given in reference. ^dRevised vinyl thermochemistry presented in reference has been used in the present work. ^eSpecies identification: *o*-C₅H₄N, *o*-pyridyl; C₅H₄N, *m*- and *p*-pyridyls; VA, vinylacetylene; CVA, cyanovinylacetylene; BZN, benzonitrile; C₃H₄, allene and propyne; C₄H₄CN, HC=CH-CH=CHCN. "l-" denotes open-chain radical. *c*-C₄H₃NMe = methylpyrrolyl.

and intermediates, the results in Table III should be considered qualitative rather than quantitative. This fact is particularly true for portions of the model that are speculative. For the main reaction sequence which is considered less speculative, the sensitivity analysis indicates that the reactions most important to the decay of the reactant and formation of major products are reactions 1, 4, 5, 6, and 7. The low sensitivity to *k*₃ (the sensitivity coefficient for all the species listed in Table III to this rate constant was less than 10⁻⁴) indicates that, at least for the value of *k*₃ estimated in this work, reaction 3 is not a rate-limiting step to

thermal decomposition of pyridine; rather, it is the production of the *o*-pyridyl radical via reaction 6 (at 1600 K) which is rate limiting. At lower temperatures (1300–1400 K), the value of the sensitivity coefficient for the pyridine concentration with respect to *k*₁ (at 100 μs) is a factor of 4 greater than for that with respect to any other rate constant. Under these conditions, reaction 1 is a rate-limiting step for the formation of *o*-pyridyl as well as for the overall decomposition of pyridine.

Our optimized value of the rate constant, *k*₁ = 10^{15.9±0.4} exp(-98 ± 3 kcal mol⁻¹/RT) s⁻¹, is in excellent agreement at 1700 K with

TABLE III: Sensitivity Coefficients in the Pyridine System for Selected Major Products Evaluated at 1600 K and at 100 μ s

reaction no.	normalized sensitivity coefficients								
	C ₅ H ₃ N	C ₂ H ₂	H ₂	HCN	HC ₃ N	C ₄ H ₂	C ₄ H ₄	CH ₄	C ₆ H ₆
1	-0.054	0.166	0.165	0.165	0.173	0.160	0.156	0.393	0.274
4	-0.040	0.164	0.125	0.067	0.213			0.290	0.180
5			0.108	-0.111	0.160				
6	-0.067	0.254	0.345		0.491			-0.555	-0.313
7	-0.044	0.117	0.109	0.350	-0.104	0.432	0.229	-0.277	
9	-0.015	0.044		0.060		0.063			
10	-0.010			0.150	-0.113	0.191	0.113		
11	-0.014		0.087		0.140			0.115	
15		0.048	-0.090	0.111	-0.133				
16									
22							0.225		
23							0.324		
24							0.179		
28				0.047	-0.055	0.104			
29								0.734	
30	0.011	-0.051	-0.081	-0.050				0.326	0.351
31	0.012	-0.055	-0.088	-0.054	-0.058			0.344	0.378
33							0.116		-0.358
35									
36		-0.081	0.084			-0.066			
37		0.084				0.354	-0.185		
38						-0.161	-0.088		
39						0.090			
42						-0.137			
45	0.003							0.260	
47								0.151	
51									0.078
52									0.392
56									0.132
									-0.367

the limiting high-pressure rate constant obtained by Leidreiter and Wagner¹⁰ for disappearance of pyridine. Our value differs from theirs by less than 5% at this temperature, and both sets of Arrhenius parameters agree well within experimental error. Thus, based on Leidreiter and Wagner's¹⁰ falloff calculations we may assume that under our experimental conditions (≈ 10 atm pressure) the unimolecular decomposition of pyridine was taking place at or very close to the high-pressure limit and that Leidreiter and Wagner's¹⁰ rate constant for disappearance of pyridine may be equated with our value of k_1 , rate constant for the fission of the ortho hydrogen of pyridine.

The reaction mechanism of Table II contains several other pressure-dependent rate constants. Some of these reactions may be in the falloff region and the rate constants for these reactions may therefore be specific for the present conditions.

Our values of k_1 and k_2 (Table II) imply experimental heats of formation for *o*-pyridyl radical of $\Delta H_f^\circ = 82 \pm 6$ kcal mol⁻¹ and for *m*- and *p*-pyridyls of 86 ± 6 kcal mol⁻¹. The latter value just encompasses the thermochemical estimate (Table I) within its error limits; however, the difference in heats of formation of *o*- and the *m*- and *p*-pyridyls is larger than the thermochemical estimate.¹⁰ An ortho stabilization energy as large as 4 kcal is, however, predicted by ab initio molecular orbital calculations on *o*-pyridyl³⁰ in which there is appreciable stabilizing interaction between the nitrogen nonbonding orbital and the singly occupied molecular orbital on the ortho carbon. This interaction is not possible for the meta and para radicals.

Our values of ΔH_f° for the pyridyls are also larger but within uncertainties of 76 ± 10 kcal mol⁻¹ obtained as an average value for the pyridyls by Kern et al.⁹ using an RRKM extrapolation of their rate data. However, in view of the possible effects of trace impurities, uncertainties in single-pulse shock tube measurements at large extent of conversion, and the additional possibility that the reaction might still be in the falloff region, we cannot yet positively reject the thermochemical estimates of $\Delta H_{f,300}$ for the pyridyls in favor of our experimental values.

Our kinetic model when applied directly to simulate the TOF profiles of Kern et al.⁹ overpredicts the rates of decomposition

of pyridine and formation of C₂H₂, although its prediction of HCN rates is in agreement. Since our model was developed for a higher range of pressures and in view of the likelihood that the unimolecular initiation reactions 1 and 2 are likely to be well into the falloff region at their pressures, the disagreement is not surprising. The failure of Kern et al.⁹ to observe cyanoacetylene amongst their products is probably not inconsistent with our results—we estimate that at their highest temperature (2092 K) HCCCN should be only one-fifth of the concentration of HCN. At the lowest temperature of their studies (1703 K) HCCCN and HCN should be of comparable concentration. However, sensitivity problems might then obscure mass spectral detection of HCCCN, especially as pyridine itself has a strong fragment peak at 51 amu (ref 31).

Sooting Tendency of Pyridine. In many previous studies (see references in Leidreiter and Wagner¹⁰) the sooting tendencies of pyridine in flames or shock tubes have been found to be substantially less than that of other aromatics (e.g., benzene). The results of this investigation are consistent with the previous studies since (except for benzonitrile) very few species with molecular weights higher than pyridine were observed. Negligible quinoline and naphthalene were detected. Furthermore, the carbon balance was reasonable ($\pm 15\%$) considering the difficulty in measuring accurately the concentrations of pyridine and other nitrogenous species. This situation differs dramatically from the pyrolyses of toluene³² and benzene¹⁸ which exhibited carbon losses of 70%

(31) *A.S.T.M. Index of Mass Spectral Data*; ASTM: Philadelphia, 1969; p 7.

(32) Colket, M. B.; Seery, D. J. "Mechanisms and Kinetics of Toluene Pyrolysis". Poster presented at 20th Symposium (International) on Combustion, Ann Arbor, MI, 1984.

(33) McCullough, J. P.; Douslin, D. R.; Messerly, J. F.; Hossenlopp, I. A.; Kincheloe, T. C.; Waddington, G. *J. Am. Chem. Soc.* **1957**, *79*, 4289.

(34) Harland, P. W. *Int. J. Mass Spectrom. Ion Processes* **1986**, *70*, 231.

(35) Hall, H. K.; Baldt, J. H. *J. Am. Chem. Soc.* **1971**, *93*, 140.

(36) Szekely, A.; Hanson, R. K.; Bowman, C. T. *Int. J. Chem. Kinet.* **1983**, *15*, 915.

(37) Kiefer, J. H.; Kapsalis, S. A.; Al-Alami, M. Z.; Budach, K. A. *Combust. Flame* **1983**, *51*, 79.

(38) Westmoreland, P. R. *Prepr. ACS Div. Fuel Chem.* **1987**, *32* (3), 480.

(39) Payne, W. A.; Stief, L. J. *J. Chem. Phys.* **1976**, *64*, 1150.

(40) Warnatz, J. In *Combustion Chemistry*; Gardiner, W. C., Jr., Ed.; Springer: New York, 1984; p 197.

(41) Hsu, D. S. Y.; Lin, C. Y.; Lin, M. C. *Symp. (Int.) Combust. (Proc.) 20th* **1984**, 623.

(30) Kikuchi, O.; Hondo, Y.; Morishashi, K.; Nakayama, M. *Bull. Chem. Soc. Jpn.* **1988**, *61*, 291.

or more (presumably to polyaromatic species and/or soot). In addition several multiringed species were observed, e.g., indene and naphthalene.

Explanations for the different sooting characteristic of pyridine usually include the fact that with an N atom in the ring large pericondensed polyaromatic compounds cannot be formed. Based on the present experimental results, it appears that it is also difficult (although not impossible) to grow a second ring. We offer two possible explanations for this phenomenon. The most likely explanation is the short lifetime of the pyridyl radical which is less than a nanosecond at temperatures of this study. Our rate constant used in this half-life calculation, is based on the endothermicity of reaction 3 and a selection of 10^{14} for the A factor. Although the model calculations were insensitive to this rate constant, we estimate a potential uncertainty of up to 1.5 orders of magnitude. In comparison, the half-life of the phenyl radical is about $50 \mu\text{s}$ (or $500 \mu\text{s}$ using the recent rate data of Braun-Unkloff et al.¹⁹ at 1500 K). Phenyl radical, in turn, is believed to be a critical intermediate leading to the growth of polyaromatic hydrocarbons. The calculated lifetime of *o*-pyridyl is unlikely to

be in error by as much as 4 orders of magnitude and so we conclude that its relatively short lifetime prevents it from playing a critical role in the growth of two-ringed species. (The other pyridyls will attain larger concentrations but due to rapid interchange with *o*-pyridyl, their concentrations will also be low.) A second more speculative explanation relates to the relative reactivity of the carbon atoms on pyridine. We speculate that the carbon atom with the lowest reactivity is located at the meta position. Analogous to the growth mechanism for polyaromatic hydrocarbons, acetylene will add to pyridyl but specifically to *o*-pyridyl or *p*-pyridyl. An addition of a second acetylene and subsequent ring closure will be inhibited since external bonding to the N atom will result in the loss of aromaticity and since the meta carbon is relatively unreactive. Growth to form a two-ringed compound will therefore be suppressed relative to that for a pure hydrocarbon.

Acknowledgment. We thank Drs. D. Seery and J. D. Freihaut for helpful discussions. D. Kocum, (UTRC) and M. Esler (University of Sydney) are also thanked for their technical and research assistance with experiments. J.C.M. gratefully acknowledges the assistance and encouragement of United Technologies Research Center through the agency of Drs. J. D. Freihaut and D. Seery whilst on leave from the University of Sydney on a Special Studies program.

Registry No. Pyridine, 110-86-1.

(42) Tsang, W. In *Shock Waves in Chemistry*; Lifshitz, A., Ed.; Marcel Dekker: New York, 1981; p 60.

(43) Kiefer, J. H.; Mizerka, L. J.; Patel, M. R.; Wei, H.-C. *J. Phys. Chem.* **1985**, *89*, 2013.

(44) Organ, P.; Mackie, J. C. To be submitted for publication.

Kinetics of Reduction of Iodine by Oxalate and Formate Ions in an Aqueous Solution. Difference in Mechanisms of the Reactions of Oxalate and Formate Ions with Iodine

Masaru Kimura,* Hitoe Ishiguro, and Keiichi Tsukahara

Department of Chemistry, Faculty of Science, Nara Women's University, Nara 630, Japan

(Received: June 23, 1989; In Final Form: December 6, 1989)

Kinetics of the reduction of iodine by oxalate and formate ions have been studied in an aqueous solution. The reduction of iodine by the oxalate ion did not occur at all in the dark but proceeded greatly by irradiation with visible light of solution. The photosensitized reaction was inhibited by the addition of acrylonitrile and acrylamide as radical scavengers. The rate of reaction was of half-order in both the concentrations of iodine and the intensity of light irradiated. The rate also increased with increasing pH at pH 3-5 and was proportional to concentrations of sodium oxalate added up to 0.1 mol dm^{-3} . Iodide ions inhibited the reaction. These results show that the photoreaction of iodine with oxalate proceeds by the dissociation of iodine to iodine atom by light. On the contrary, iodine was reduced by the formate ion in the dark, being indifferent to the intensity of light irradiated. The reduction of iodine by formate was not inhibited at all by the radical scavengers of acrylonitrile and acrylamide. The rate was proportional to the concentrations of sodium formate but was inversely proportional to those of iodide. The reactive species are not I_3^- and HCOOH but are I_2 and HCOO^- . The mechanisms of reaction of formate are completely different from those of oxalate: the former is a thermal and bimolecular reaction, while the latter is a light-induced and radical reaction containing $\text{CO}_2^{\cdot-}$ and $\text{I}_2^{\cdot-}$.

Introduction

Both oxalate and formate ions are two-electron reductants with the standard oxidation potentials (E°) being 0.49 and 0.196 V vs NHE for reactions $\text{H}_2\text{C}_2\text{O}_4(\text{aq}) = 2\text{CO}_2 + 2\text{H}^+ + 2\text{e}^-$ and $\text{HCOOH}(\text{aq}) = \text{CO}_2 + 2\text{H}^+ + 2\text{e}^-$, respectively.¹ Therefore, oxalate is a much stronger reductant than formate, and the oxidation of oxalate is in general much faster than that of formate in acidic solutions. For example, in our recent study,² the second-order rate constants at 25 °C for the oxidations of oxalate and formate ions by tris(2,2'-bipyridine)ruthenium(III) ions were 1.1×10^4 and $0.144 \text{ dm}^3 \text{ mol}^{-1} \text{ s}^{-1}$ (at pH 3.2-3.7), respectively. We have been interested in the reactivity difference of the oxalate and formate ions with respect to the mechanisms of electron-

transfer reactions. Recently, the kinetic determination of trace amounts of nitrite ion was reported³ based on its inhibitory effect on the photochemical reaction between ethylenediamine-*N,N,N',N'*-tetraacetic acid (EDTA) and iodine. The mechanisms of reaction between EDTA and iodine appeared complex, and there remained an unanswered problem. Both oxalate and formate ions are simple compounds and favorable for elucidating mechanisms of such reactions with iodine.

Experimental Section

Chemicals. Sodium oxalate, sodium formate, iodine, potassium iodide, and other chemicals used were of guaranteed reagent grade from Wako Pure Chemical Industries, Ltd. All solutions were prepared from redistilled water. The pH of the solution was

(1) Latimer, W. M. *Oxidation Potentials*, 2nd ed.; Prentice Hall: New York, 1952.

(2) Nishida, S.; Kimura, M. *J. Chem. Res., Synop.* **1986**, 336.

(3) Sanchez-Pedreno, C.; Sierra, M. T.; Sierra, M. I.; Sanz, A. *Analyst* **1987**, *112*, 837.